Lecture 11

Chemical State Imaging for Investigations of Neurodegenerative Disorders: Chemical State of Iron in Parkinsonism Dementia Complex (PDC)

11.1. Experimental Procedure and Results

In another study, Fujisawa et al. (2002) applied XRF and XANES to the substantia nigra from the same samples, namely post-mortem tissues of a patient with Parkinsonism-dementia complex (PDC) and a control subject, and carried out chemical state imaging which differentiates between Fe^{2+} and Fe^{3+} in iron components. This work is discussed in detail in the following. For reference in the XANES analyses, they used FeO (99.9 % purity) from High Purity Chemetals Laboratory Ltd. and and Fe_2O_3 powders (98 % purity) from Wako Pure Chemical Industries Ltd.

The measurements were performed in vacuum, at beam line 39XU of SPring-8, Japan Synchrotron Radiation Research Institute (JASRI). Monochromatic incident photon beams were restricted by a set of *x*-*y* slits and a pinhole to produce about a beam 10 μm in diameter.

XRF analyses were performed for elemental mapping. Fluorescent x-rays were collected by a solid state detector (SSD). Fe K-edge XANES analyses were performed in the energy range of 7.100 to 7.160 keV at 0.5 eV intervals. The data were measured in fluorescence mode for biological specimens and in transmission mode for the reference samples. Incident and transmitted photon flux was monitored with an air-filled ion chamber. Fe K-edge fluorescent x-rays were also collected by a solid state

detector (SSD).

In the XANES measurement, the incident energy near the absorption edge is chosen so that selective excitation of specific chemical species will occur. XANES spectra of FeO (Fe^{2+}) and Fe_2O_3 (Fe^{3+}) (reference materials) are shown in figure 11.1. At 7.16 keV energy, above the absorption edge, both Fe^{2+} and Fe^{3+} are excited. At 7.12 keV energy, near absorption edge, Fe^{2+} is selectively excited and the excitation of Fe^{3+} is suppressed. Since fluorescent x-rays are emitted accompanied with the excitation of the absorbing elements, XRF imaging that distinguishes chemical state can be obtained because of the sensitivity of the x-ray absorption coefficient to the chemical state [1, 2].

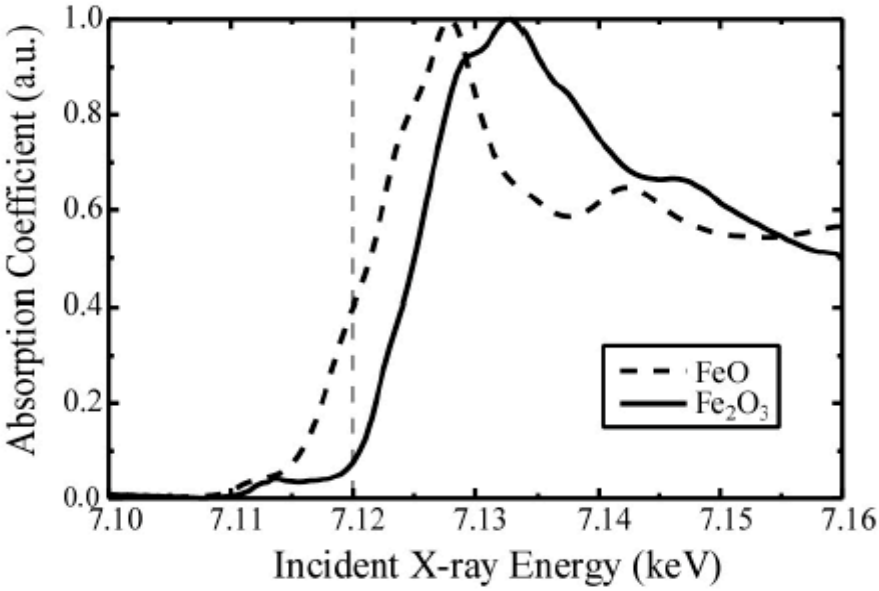

Figure 11.1. X-ray absorption fine structure (XAFS) spectra of FeO (Fe^{2+}) and Fe_2O_3 (Fe^{3+}).

Fujisawa et al. used the following procedure to obtain chemical state imaging. First, XRF imaging was performed with the incident x-ray energy at 7.160 keV (above the edge) and at 7.120 keV (near the edge). Then the yields of Fe^{2+} and Fe^{3+} were derived using the XRF yields of each point and the absorption coefficients at incident

energies of 7.160 keV and 7.120 keV (Table 11.1).

Table 11.1. X-ray absorption coefficient of FeO (Fe^{2+}) and Fe_2O_3 (Fe^{3+}) at the incident energy of 7.160 keV and 7.120 keV

	7.160 keV	7.120 keV
Fe_2O_3 (Fe^{3+})	0.498	0.075
FeO (Fe^{2+})	0.565	0.399

The results of the XRF analyses on substantia nigra tissues of a PDC case and a control case from this work are shown in figure 11.2. The optical microscopic photograph of the double-stained tissue (hematoxylin-eosin Bodian to determine cell type and neurofibrillary tangles) and XRF imaging of iron in the PDC tissues are shown in figures 11.2a and b, respectively. Two neuromelanin granules released from dead neurons and some glial cells surrounding the neuromelanin are observed. As in Shikine et al. study reported above, iron concentrations are detected in the neuromelanin granules and one of the glial cells. Chemical state imaging which separates Fe^{2+} and Fe^{3+} concentrations was performed in the same area of the PDC tissue (figure 11.2c,d). Distributions of Fe^{2+} and Fe^{3+} were well distinguished in the PDC tissue. Fe^{2+} concentration is observed in the neuromelanin, and Fe^{3+} concentration is observed in the glial cell. In the glial cell, Fe^{3+} concentration is at a high density, while the Fe^{2+} is low. This indicates that Fe^{3+} is the predominant valence state of iron contained in the glial cell.

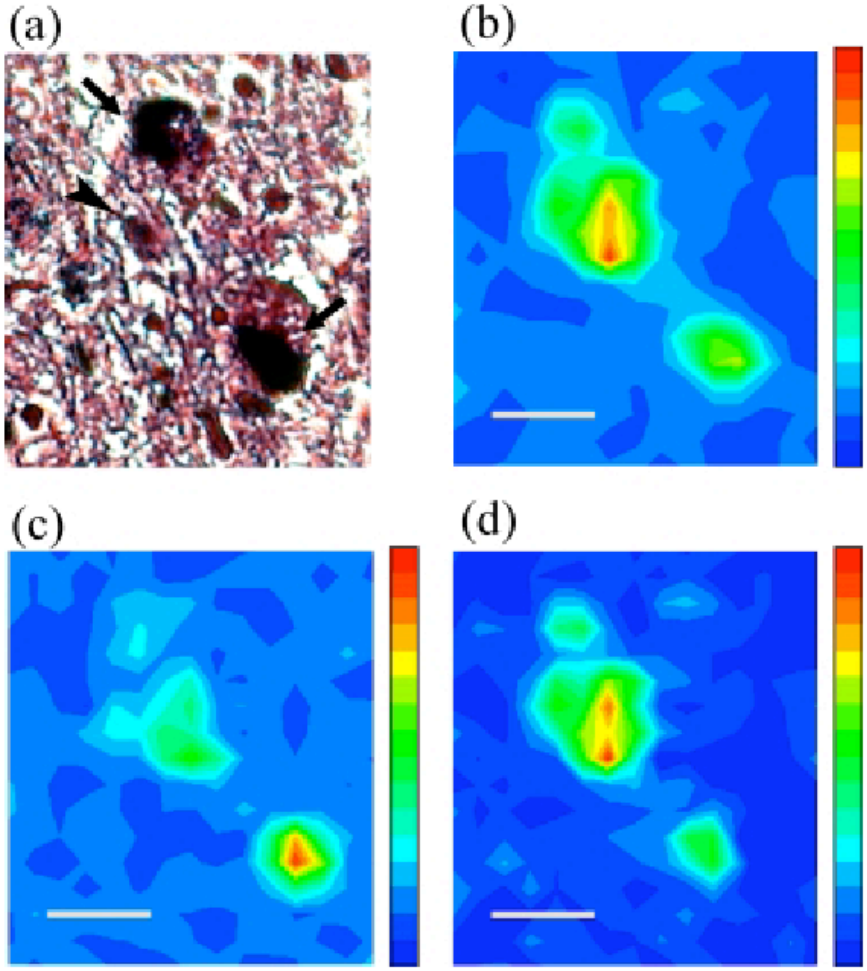

Figure 11.2. XRF imaging of substantia nigra tissue from a Parkinsonism-Dementia complex case. The measurement area was 70 × 80 μm, and was divided into 14 × 16 pixels. (a) Optical microscope photograph of the measurement area taken after x-ray analysis. Arrows indicate neuromelanins and an arrowhead indicates a glial cell, where iron accumulation was observed. (b) X-ray fluorescence imaging of yield of iron. The range of the fluorescent x-ray intensity is from 0 to 22 counts per second. (c) Chemical state imaging of Fe^{2+}. (d) Chemical state imaging of Fe^{3+}. The range of the density is from 0 to 40 for Fe^{2+}, from 0 to 60 for Fe^{3+} (arbitrary unit). Scale bars are 20 μm.

The optical microscopic photograph and XRF imaging of iron in tissue from the control subject are shown in figures 11.3a and b, respectively. Several nigral neurons containing neuromelanin can be observed. Iron concentrations were readily detected in these neuromelanins. The chemical state imaging in the same area of the control tissue is shown in figures 11.3c,d. The distributions of Fe^{2+} and Fe^{3+} in melanized neurons

were similar to that of control. Again, in the control tissues, iron components in the melanized neurons were mixed states of Fe^{2+} and Fe^{3+}.

Fe K-edge XANES analyses were applied to selected points where high iron concentrations were detected in the tissues in order to analyze chemical states in detail. Figure 11.4 shows the XANES spectra in the tissues and those of reference samples (FeO and Fe_2O_3). Measurement points are in the melanized neuron of control, the neuromelanin granule and the glial cell of the PDC tissue. The ordinate and abscissa represent the absorption coefficient and incident x-ray energy, respectively. The spectra were normalized by the absorption jump, defined as the difference between the highest and the lowest point in each spectrum. The absorption edge is defined at the half-height of the absorption jump.

From spectra of figure 11.4 the chemical shifts of iron contained in neuromelanin of the PDC case and the control case are deduced to be 1.1 eV and 1.8 eV respectively, from that of Fe^{2+} in FeO. For the glial cell of the PDC case is 3.5 eV. This is close to the chemical shift of Fe^{3+} from Fe_2O_3 of about 3.7 eV. The absorption edge of the iron contained in the neuromelanin within the PDC and the control tissues are mixed states of Fe^{2+} and Fe^{3+}. In comparison with the absorption edge of the iron in the neuromelanin of the PDC and the control case, the chemical state of the iron contained in the neuromelanin within the PDC and the control tissue are almost similar. These results are in accordance with the chemical state imaging.

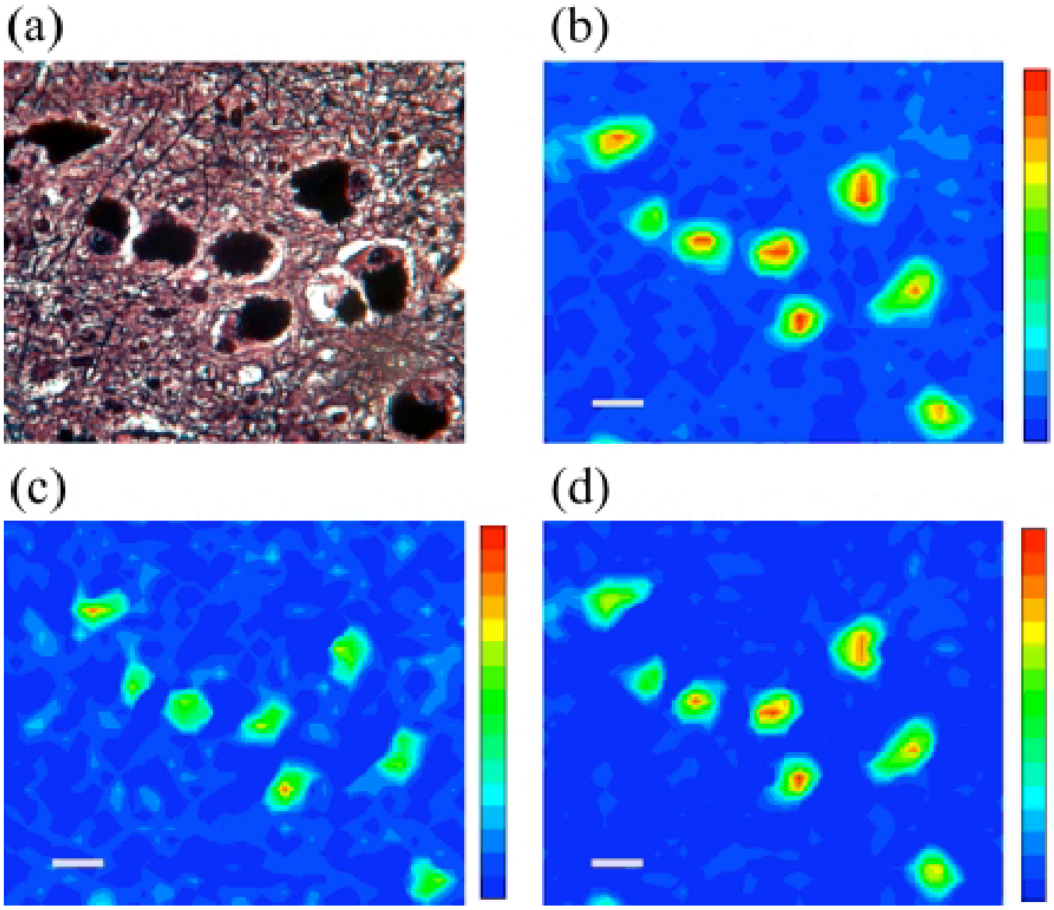

Figure 11.3. XRF imaging of substantia nigra tissue from a control case. The measurement area was 180 × 150 μm, and was divided into 36 × 30 pixels. (a) Optical microscope photograph of the measurement area taken after x-ray analysis. (b) X-ray fluorescence imaging of yield of iron. The range of the fluorescent x-ray intensity is from 0 to 18 counts per second. (c) Chemical state imaging of Fe^{2+}. (d) Chemical state imaging of Fe^{3+}. The range of the density is from 0 to 25 for Fe^{2+}, from 0 to 70 for Fe^{3+} (arbitrary unit). Scale bars are 20 μm.

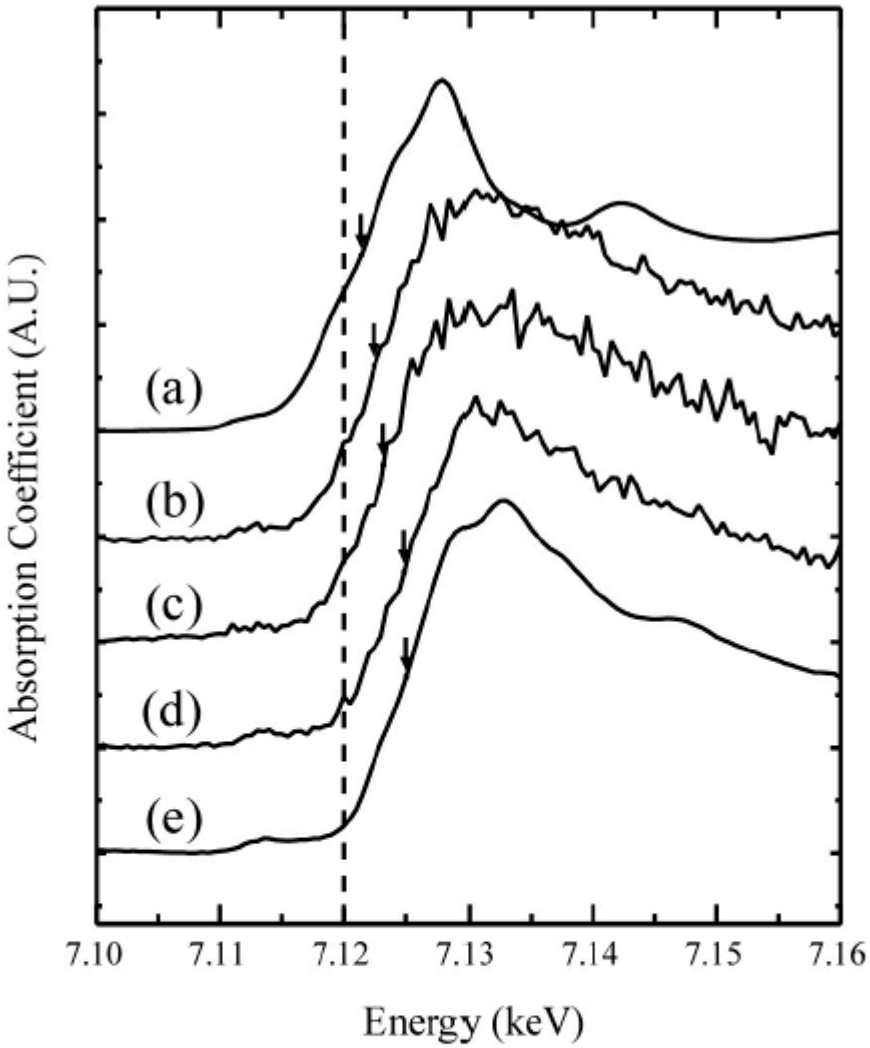

Figure 11.4. Fe K-edge XANES spectra of (a) FeO powder, (b) the neuromelanin granule from the PDC case, (c) the neurolemanin granule from the control case, (d) one glial cell from the PDC case, and (e) Fe_2O_3 powder. Arrows indicate the absorption edge. The incident beam size was about 10 μm in diameter for (b)-(d).

11.2. Quantitative analyses and Fe^{3+}/Fe^{2+} ratio

Quantitative analysis of the concentrations of iron and other elements contained in the PDC and control tissues was performed. The quantitative analysis was applied to the nigral neurons which has neuromelanin granules, one of glial cells and matrix in the tissue of PDC and control (table 11.2). The concentrations of iron in the nigral neurons with PDC are 1000 ~ 3700 ppm, which is higher than those in the control nigral neurons

800 ~ 2000 ppm. This result indicates that nigral neurons with PDC have iron accumulation compared to those with control. The increase of Cr and Mn also can be seen in PDC nigral cells.

In order to obtain the Fe^{3+}/Fe^{2+} ratio of iron contained in the tissues, XRF analysis was performed at several points in PDC nigral tissues of a patient at two incident x-ray energies of 7.160 keV and 7.120 keV. An optical microscopic photograph of the tissue is shown in figure 11.2, where some neuromelanin granules and glial cells can be seen. Typical XRF spectra in the tissue are shown in figure 11.5. The ordinate and abscissa represent XRF intensity and fluorescent energy, respectively. XRF intensity is normalized using fluorescent intensity divided by I_0. I_0 is the incident x-ray intensity, propotional to photons per second, measured by ionized chamber. Table 11.3 shows the XRF yield of iron at several points in the tissue where iron was detected with high density, at neuromelanin granules and one of the glial cells. The Fe^{3+}/Fe^{2+} ratio is obtained using XFR yield and absorption coefficient (table 11.1). We can see that Fe^{3+}/Fe^{2+} ratio varies at the points in the tissues. For example, Fe^{3+}/Fe^{2+} ratio of iron contained in the glial cell is about ten times higher than that in the neuromelanin granule (A). Chemical state of iron can be well distinguished at the different points in the tissues.

Table 11.2. Concentrations of the elements in the PDC tissues and the control tissues. The unit is ppm. The density of the tissues is assumed to be 1.0 g/cm^3.

		P	S	Cl	Ca	Cr	Mn	Fe
PDC	neuron	3168.2	8806.9	1027.6	430.9	83.8	142.6	3754.9
	neuron	1917.1	8476.0	826.4	248.1	52.8	134.5	3165.6
	neuron	1237.0	3291.5	311.7	175.6	50.8	91.5	1018.5
	neuron	1935.9	6752.1	661.5	245.7	68.5	112.5	2621.7
	glial cell	1106.9	1927.7	292.7	167.8	37.5	181.4	3828.7
Control	neuron	1644.7	4567.2	542.7	405.6	6.7	21.5	962.8
	neuron	1865.5	5577.0	458.9	638.6	20.7	16.5	845.4
	neuron	2097.5	5891.4	640.3	472.3	1.7	12.0	1487.0
	neuron	1940.4	4258.0	439.3	412.8	14.2	20.8	815.2
	neuron	1801.5	4451.4	630.8	334.3	-	10.3	1061.6
	neuron	2468.3	7343.7	682.7	505.7	12.3	29.0	1933.0
	neuron	1799.5	5119.8	469.5	297.3	8.1	12.6	1166.4
	neuron	1247.2	5531.4	465.8	424.2	7.7	17.1	1959.2
PDC	matrix1	809.5	1835.0	114.6	113.0	-	56.6	365.2
	matrix2	462.2	1913.2	139.2	345.5	24.6	47.5	401.0
	matrix3	458.3	1294.0	106.5	330.0	20.0	74.0	484.5
Control	matrix1	1467.6	3267.2	264.9	340.4	-	15.5	164.4
	matrix2	1815.9	2660.4	339.3	241.4	8.7	-	305.2

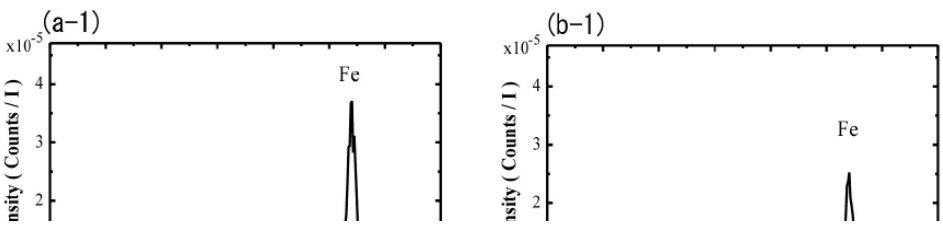

Figure 11.5. Typical XRF spectra in the tissue with PDC. Measurement points were inside of glial cell and neuromelanin granules. (a-1) Glial cell, incident energy of 7.160 keV. (a-2) Glial cell, 7.120 keV. (b-1) Neuromelanin granules, 7.160 keV. (b-2) Neuromelanin granules, 7.120 keV. Measurement time was 200 seconds for each point.

Table 11.3. Peak area of x-ray fluorescence spectra in the tissues of PDC with the incident energy of 7.160 keV and 7.120 keV. Measurement time was 200 seconds for each point. XRF yields was normalized by incident x-ray intensity.

Target	XRF yield (7.160keV)	XRF yield (7.120keV)	Fe^{3+}/Fe^{2+}
Grial cell	3.98E-05	9.81E-06	5.46
Neuromelanin(A)	2.60E-05	1.42E-05	0.47
Neuromelanin(B)	1.03E-05	2.94E-06	3.55
Extra cellar tissue	5.17E-06	1.90E-06	1.77

11.3. Discussions and summary

In this work chemical state analyses were applied to pathological tissues. Chemical state imaging which separates Fe^{2+} and Fe^{3+} was obtained with the following assumptions: 1) the absorption coefficient curve of different valence states of iron (Fe^{2+} and Fe^{3+}) was represented by only iron oxide (FeO and Fe_2O_3), 2) iron contained in the

tissues is a superposition of Fe^{2+} and Fe^{3+}. It should be noted that these assumptions are too simplified to represent the complex system, which contains chlorine and other compounds of Fe. These assumptions may be justified considering the important role of oxides of iron in oxidation and reduction activities of brain. Under these assumptions, the chemical states of iron contained in the tissues were well distinguished.

XRF analyses revealed an excessive accumulation of iron in the neuromelanin granules of the PDC tissues. This result is in good agreement with previous studies which show iron concentration in neuromelanin in tissues from PD cases [3, 4]. In this study, iron contained in the neuromelanin of the PDC and the control cases are mixed states of Fe^{2+} and Fe^{3+}. In a patient with PD, selective vulnerability can be seen in melanized neurons [5, 6], so there are several hypotheses that suggest that neuromelanin may be part of what is responsible for neuronal degeneration [7]. The chemical state of the iron in dopaminergic neurons is important in understanding the role of iron in the pathogenesis.

In this study, high accumulation of iron can be seen in one of glial cells near the neuromelanin granules in the PDC tissue. In this area, the chemical state of iron has shifted toward Fe^{3+}. In the previous study [8], high accumulation and chemical shifts of iron were found in some of the glial cells of a PD case. McGeer reported that numerous microglia or macrophages phagocytosed dopaminergic neurons in SN pars compacta of post-mortem parkinsonian brains [9, 10]. This can be related to excessive accumulation of iron, specially, iron in the higher charge state (Fe^{3+}). These results (Fujisawa et al. 2002) also show excessive accumulation and significant chemical shifts of iron in one of the glial cells. This can be related to an important aspect of the role of iron in glial cells of PDC and PD cases.

The XANES spectra of iron contained in the tissues were not smooth. In the beam and tissue interaction region, an estimate of the physical parameters showed that the volume the tissues was about 600 μm^3 and weight was 600 pg (pg = 10^{-12} g), and the iron content in the tissue was about 2.5 pg [11]. A typical value for the detection limit [12] obtained by using the signal/noise ratio in a typical spectrum was 0.1 pg. The XANES spectrometry using micro beam was performed for the iron contents of a few pg or less. The practical measurement time at each point was about 50 to 60 seconds, and the total measurement time for each spectrum was about 2 hours. The fluctuation in the XANES spectra of trace elements in the tissues is inevitable when using SR micro beams for practical applications.

In this study chemical state imaging of iron could clearly discriminate between tissues containing mainly Fe^{2+} and tissues containing Fe^{3+} from the PDC case and the control. This method can be used to help us understand the behavior of transition metals inside and outside cells, and can be used widely for investigations in neurology, basic cell biology and pathological fields.

11.4. Conclusion

In this chapter, application of SR methods demonstrated a novel approach to the study of biological function of cells through the investigation of the intracellular elemental conditions with high spatial resolution and sensitivity. Micro-XRF and XANES analyses are ideal techniques for providing the distributions, concentrations and chemical states of trace elements. Furthermore, their non-destructive nature allows histological analysis of the samples by staining after the elemental analysis. These features can not be obtained by the conventional techniques and were exploited in the

present study. The analyses enable the absolute concentrations of a wide range of the trace elements to be determined. This quantitative information is of significant importance for elucidating the role of intracellular trace elements in the investigation of biomedical samples.

The case study of parkinsonism-dementia complex (PDC) revealed that the substantia nigral tissue obtained from the PDC case showed the decrease of Zn and accumulation of Fe. These may be the direct evidence of cytotoxicity from oxidative stress and tyrosine nitration. The accumulation of As contents that is strongly toxic for tissues was also found in the PDC case. It was clarified that the phagocytosis by the glial cell had occurred.

There is no doubt that micro-XRF and XANES analyses will provide unprecedented opportunities to analyze biological samples in future studies as well as the present work. The quantitative information at this level is not accessible with more traditional imaging and spectroscopic method and will contribute to the development of therapy of neurodegenerative disorders.

References

1. K. Sakurai, A. Iida, Y. Gohshi, *Adv. in X-ray Anal.,* **1989**, 32, 167.
2. H. Ade, X. Zhang, S. Cameron, C. Costello, J. Kirz, S. Williams, *Science,* **1992**, 258, 972
3. A.M. Ektessabi, S. Yoshida, K. Takada, *X-ray Spectrom.,* **1999**, 28, 456.
4. L. Zecca, T. Shima, A. Stroppolo, C. Goj, G.A. Battiston, R. Gerbasi, T. Sarna, H.M. Swartz, *Neuroscience*, **1996**, 73, 407.
5. E.C. Hirsh, A. Graybiel, Y. Agid, *Nature,* **1988**, 334, 345.
6. W.R. Gibb, *Brain Res*., **1992**, 581, 283.
7. Kastner, E.C. Hirsh, Q. Jejeune, F. Javoy-Agid, O. Rascol, Y. Agid, *J. Neurochem*., **1992**, 59, 1080.
8. S. Yoshida, A.M. Ektessabi, S. Fujisawa, *J. Synchr. Rad.,* **2001**, 8, 998.
9. P.L. McGeer, S. Itagaki, B.E. Boyes, E.G. McGeer, *Neurology,* **1988**, 38, 1285.
10. P.L. McGeer, S. Itagaki, H. Akiyama, E.G. McGeer, *Ann. Neurol.,* **1988**, 24, 574.
11. A.M. Ektessabi, S. Shikine, S. Yoshida, "*Application of Accelerators in Research and Industry"- Sixteenth Int'l Conf.*, ed. J.L. Duggan and I.L. Morgan, **2001**, 720.
12. C.J. Sparks Jr., "*Synchrotron Radiation Research*", **1980**, ed. H. Winick and S. Doniach, Plenum Press.